TTT and CHT Curing Diagrams of Water-Borne Polycondensation Resins on Lignocellulosic Substrates

A. PIZZI, C. ZHAO, C. KAMOUN, H. HEINRICH

ENSTIB, University of Nancy 1, Epinal, France

Received 16 November 1999; accepted 22 May 2000

ABSTRACT: Lignocellulosic substrates such as wood were found to have a marked modifying influence on both lower temperature and higher temperature zones of TTT and CHT diagrams during hardening of phenol–resorcinol–formaldehyde (PRF) and melamime–urea–formaldehyde (MUF) polycondensates. Although the modifying influence of the substrate on the higher temperature zone of CHT diagrams presented the same trend of what was already reported for phenol–formaldehyde (PF) and urea–formaldehyde (UF) polycondensates, marked differences from what reported in the literature were recorded for TTT diagrams of all these polycondensates as well for the lower temperature zones of the CHT diagrams on lignocellulosic substrates, both of which had not been investigated previously. The chemical and physical mechanisms of the interactions of the resins, the substrate, and the water carrier causing such marked variations are presented and discussed. Although in the higher temperature zones both substrate and water carrier play an important role, in the lower temperature zone the presence of water appears to be the dominant factor causing the observed variations. The generalized modified CHT and TTT diagrams characteristic of the behavior of these water-borne polycondensates on lignocellulosic substrates can be used to describe the behavior and complex changes of phase the formaldehyde-based polycondensation resins undergo when used as wood adhesives during their curing directly in the wood joint. The results also show that diagrams obtained with pure resin cannot be used to predict the behavior of the polycondensate when this is markedly modified by the presence of interacting solvents and substrates. © 2001 John Wiley & Sons, Inc. J Appl Polym Sci 80: 2128–2139, 2001

Key words: curing diagrams; water-borne polycondensation resins; lignocellulosic substrates; TTT diagram; CHT diagram; wood adhesives; substrate influence

INTRODUCTION

The concept of the isothermal time–temperature–transformation (TTT) cure diagram in which gelation and vitrification times are plotted vs. the isothermal cure temperature, is useful for understanding the behavior of thermosetting resins under isothermal cure conditions.[1] In TTT diagrams the S-shaped vitrification curve and the gelation curve divide the temperature vs. time diagram into four distinct states of matter: liquid, gelled rubber, ungelled glass, and gelled glass (Fig. 1). Analogous to the isothermal TTT diagram is the continuous heating transformation (CHT) cure diagram that reports the times and temperatures required to reach similar events during the course of continuous heating at constant heating rates (Fig. 1).[2] The gelation and vitrification curves are the most characteristic features of both TTT and CHT diagrams, the S shape of the latter in par-

Correspondence to: A. Pizzi.

Journal of Applied Polymer Science, Vol. 80, 2128–2139 (2001)

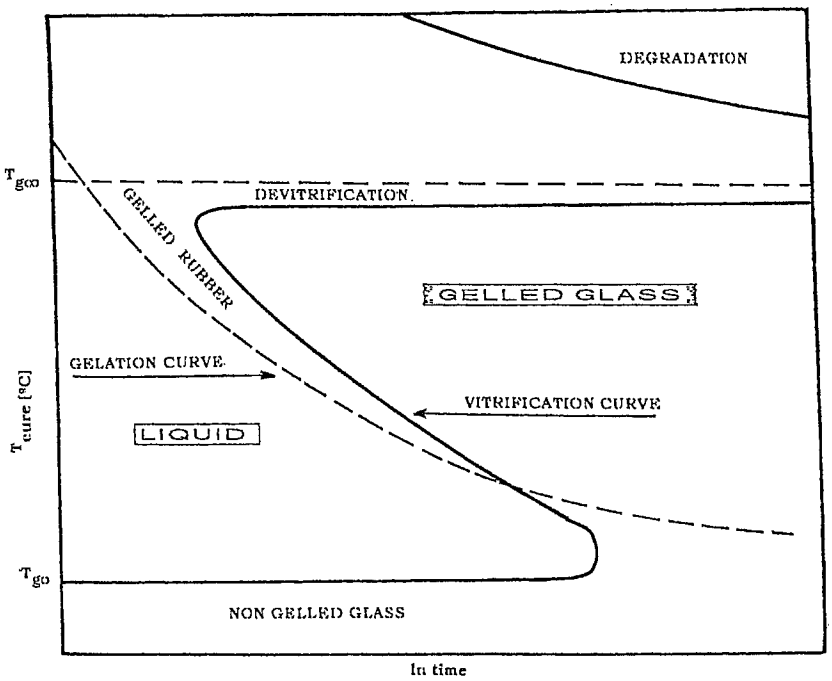

Figure 1 Nonmodified generalized time–temperature–transformation (TTT) diagram.

ticular defining the region at which the reaction rate is greatly reduced because diffusion control becomes more pronounced in the glass transition region. The CHT and TTT diagrams quantitative studies reported up to now have mostly been on the curing of epoxy resins on glass fiber braid[1–5] due to the need of defining the diagrams themselves under conditions of minimum interference between resin and substrate, and with a resin, the curing path of which is well defined and relatively straightforward.

Recently, however, CHT diagrams of other polycondensation resins used in considerable amounts as wood adhesives, namely urea–formaldehyde (UF) resins and phenol–formaldehyde (PF) resins, on a lignocellulosic substrates, namely wood, have been reported.[6] This was done because these two resins are the most used (by volume) polycondensation resins today, their main use being as thermosetting wood adhesives.[7] The presence of the lignocellulosic substrate and the fact that the resins are in water solution yielded CHT diagrams rather different than the CHT diagrams reported for epoxy resins in the absence of water and on a nonreactive substrate such as glass.[7] This study concentrated only on the higher temperature region of the diagram in which it appeared obvious that differences existed. The zone of lower temperature of the diagram was not checked because the technique used, namely thermomechanical analysis, did not allow with the limitation of equipment available to investigate the characteristics of thermosetting resins such as UF and PF resins.

To investigate the zone of lower temperature of the diagram with the rather limited capabilities of the equipment available it was necessary to use a polycondensation resin capable to cure at ambient and at lower temperature; hence, a resin presenting very high reactivity. Furthermore, to compare the results obtained with those previously obtained with UF and PF resins, such a resin should be examined on a lignocellulosic substrate, hence be a wood adhesive, as well as being a water-born resin. The resins that were chosen to correspond to such characteristics were the phenol–resorcinol–formaldehyde (PRF) and the melamine–urea–formaldehyde (MUF) resins, as both satisfy the requirements outlined. PRF resin are used industrially as cold-setting wood adhesives for structural application, and MUF resins are, among other uses, also used for such an application.

In this article are then presented the CHT and TTT diagrams obtained by TMA for both these two types of resin on a standard wood substrate

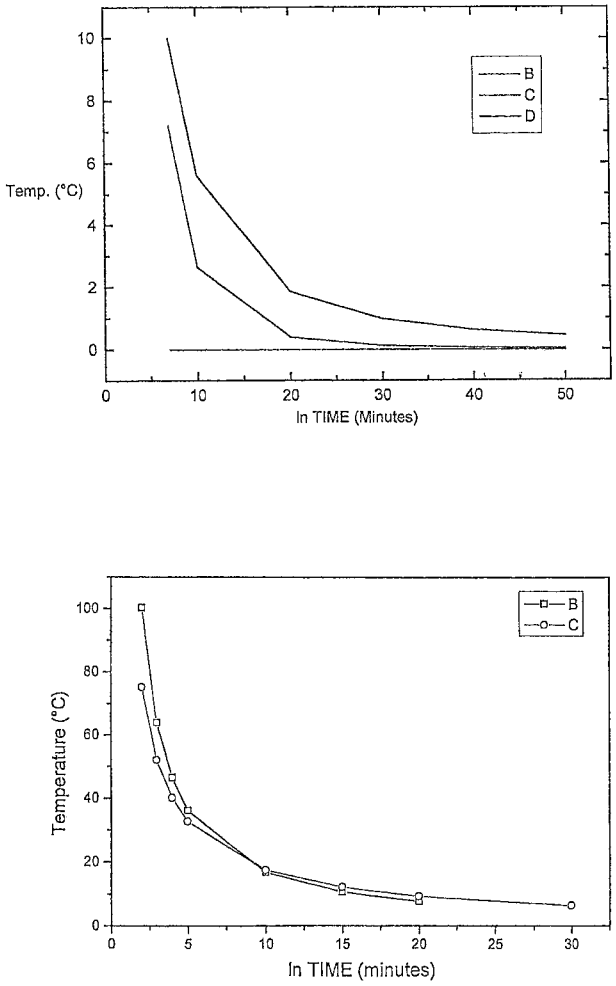

Figure 2 Lower temperature zone of the CHT diagram for lower viscosity water-borne PRF resin in a beech wood joint showing details of (a) trend to asymptotic temperature value for both gelation and vitrification curves, and (b) crossover point of gelation and vitrification curves.

(beech wood) in both the high temperature and low temperature zones of the two types of diagram.

EXPERIMENTAL

Thermomechanical Analysis (TMA) Determination of Average Number of Degrees of Freedom of Networks

Recently, work on the formation of polymer networks by photopolymerizable and polyester surface finishes on wood and of polycondensation resins used as wood adhesives has yielded a mathematical relationship[8–10] between the energy of interaction (E) at the synthetic polymer/wood interface calculated by molecular mechanics (work of adhesion), the number of degrees of freedom (m) of the segment of the synthetic polymer between two crosslinking nodes, the coefficient of branching, hence, the functionality of the starting monomer and the relative deflection (f) obtained by thermomechanical analysis (TMA) of wood specimens coated or bonded with the adhesive through the expression $f = km/E$, where k is a constant.[8–10] Regression equations[8] correlating directly to m with E and m with f have been derived for hardened phenol–formaldehyde (PF), resorcinol–formaldehyde (RF), melamine–formaldehyde (MF), and tannin–formaldehyde (TF) resins. These relationships have been used to calculate m for two commercial phenol–resorcinol–formaldehyde (PRF) resin of molar ratio total phenols: formaldehyde = 1 : 1.25, prepared by a multistep reaction procedure, at the delivered resin solids content of 53%, hardened by the addition of 16% fine paraformaldehyde powder on resin solids, and containing both organic (vegetal) flour and mineral flour fillers, and for a commercial MUF resin of 60% solids content and (M+U) : F molar ratio of 1 : 1.5, the latter catalyzed with 1.5% NH_4Cl.

To this purpose the MUF and PRF resins above were tested dynamically by thermomechanical analysis (TMA) on a Mettler apparatus. The MUF resin used was a plywood type of molar ratio (M+U) : F = 1 : 1.5 and of resin solids content equal to 60%. The PRF resin was a commercial resin for laminated wood beams of a molar ratio P : F = 1 : 1.25 and solids content equalt to 53%, and of pH 8.3, and with a total resorcinol content on liquid adhesive of 17% by weight. To this were added according to industrial formulation in one case just 8% on total liquid resin of fine paraformaldehyde powder hardener and 200 mesh wood flour and coconut shell flour fillers (50 : 50) to obtain a viscosity of the glue mix of 3000 centipoises. The second PRF resin, with a total resorcinol content of 25% by weight on liquid resin, and thickened with silica smoke (Aerosyl) was instead made by addition of its liquid industrial hardener in a weight proportion of 4 liquid resin : 1 liquid hardener, to obtain a final resin viscosity of 6000 centipoises. The MUF resin was used by addition of 1.5% on total resin solids of ammonium chloride hardener added as a 25% water solution. Samples of beech wood alone, and of two beech wood plys bonded with each system of liquid poly-

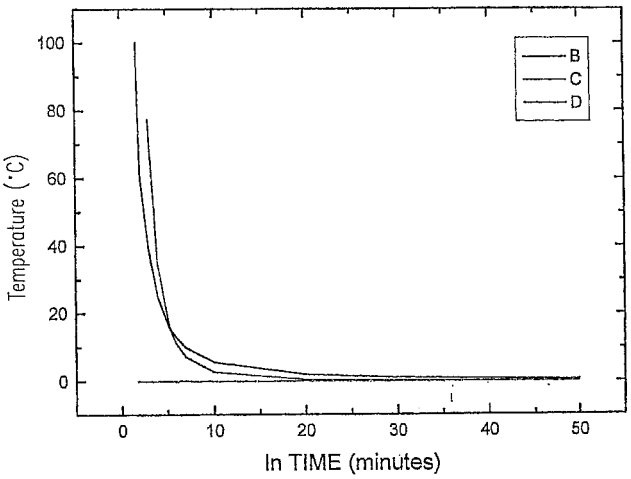

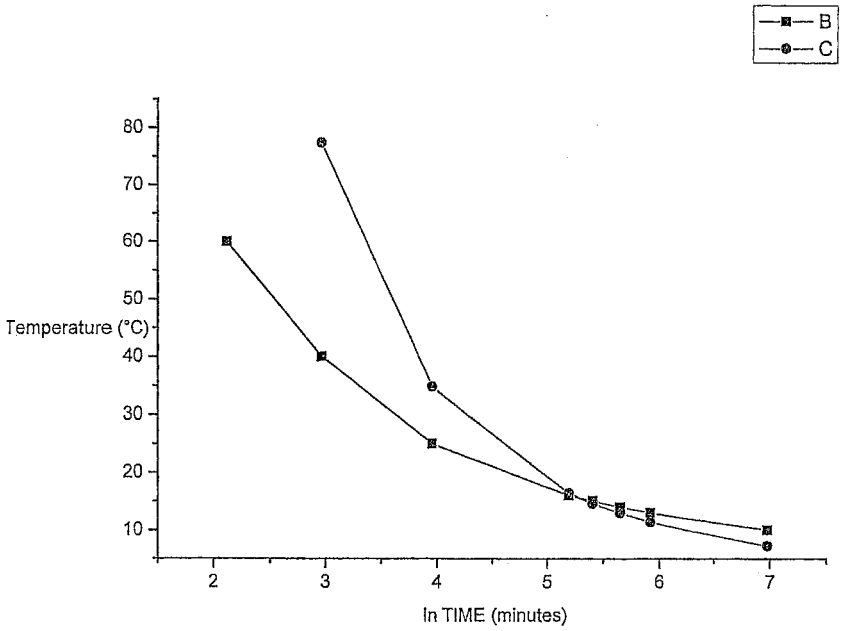

Figure 3 Lower temperature zone of the CHT diagram for higher viscosity water-borne PRF resin in a beech wood joint showing details of (a) trend to asymptotic temperature value for both gelation and vitrification curves, and (b) crossover point of gelation and vitrification curves.

condensate resins in a layer of 350 μm, for a total sample dimensions of 21 $\times$ 6 $\times$ 1.1 mm were tested (1) for the CHT diagrams in nonisothermal mode between 20 and 450°C at heating rates of 3, 5, 7.5, 10, 15, 20, 25, 30, 40, 50, 60, and 70°C/min; and (2) for the TTT diagrams by heating at a costant heating rate to a predetermined temperature and then mantaining the joints under isothermal conditions, the final temperatures being initially of 25, 40, 60, 80, 100, 120, 140, 160, and 180°C, and later at higher temperatures as indicated in the figures, with a Mettler 40 TMA apparatus in three points bending on a span of 18 mm exercising a force cycle of 0.1 *N*/0.5 *N* on the specimens with each force cycle of 12 s (6 s/6 s) and the resulting modulus curves as a function of

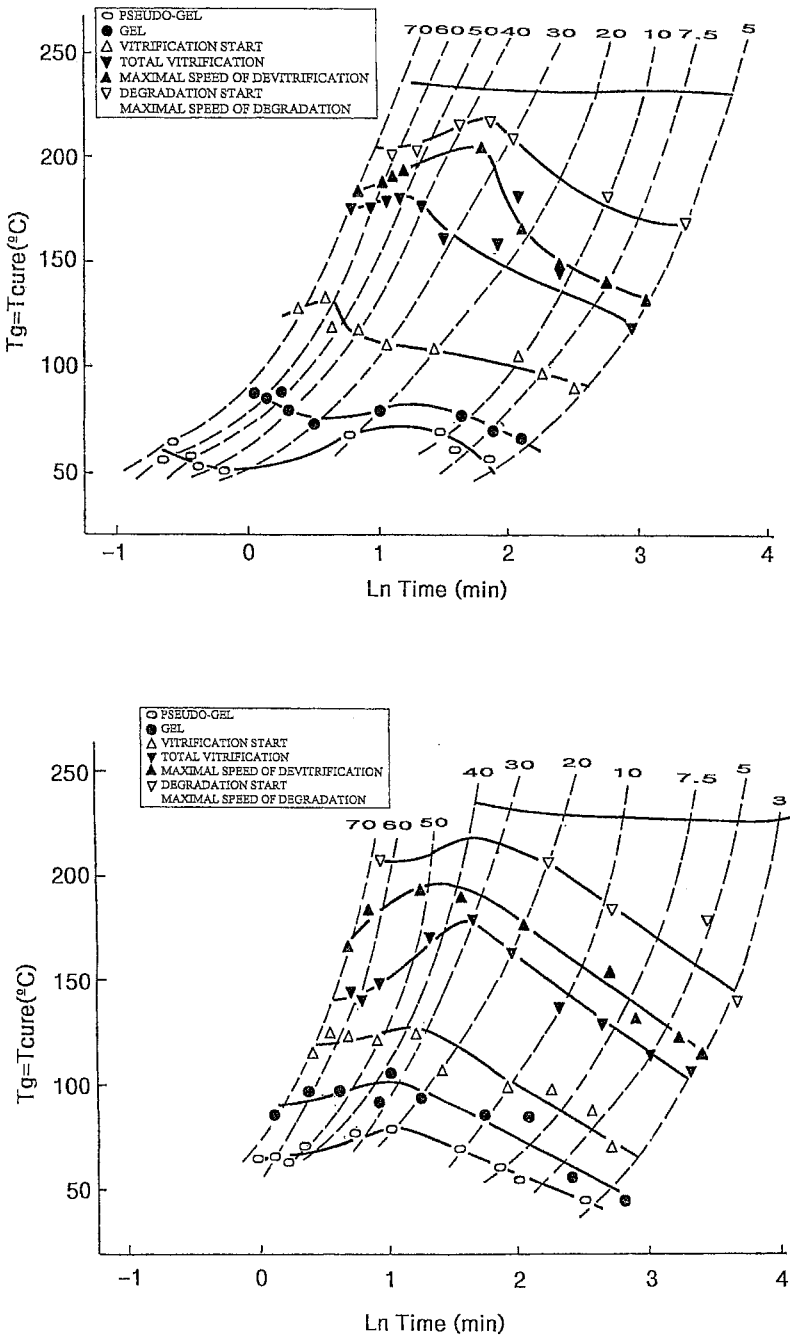

Figure 4 Detail of the modified high temperature zone of the continuous heating transformation (CHT) diagram for PRF resins on a beech wood joint. (a) lower viscosity, lower resorcinol content PRF resin, and (b) higher viscosity, higher resorcinol content PRF resin. The experimental points, the curves of the start of and total vitrification, gelation, pseudogel, start of degradation, and maximal rate of degradation and the curves connecting them at the same heating rates are indicated.

both temperature and time obtained. The classical mechanics relation between force and deflection $E = [L^3/(4bh^3)][\Delta F/\Delta f]$ allows the calculation of the Young's modulus E for each of the cases tested. As the deflections Δf obtained were proven to be constant and reproducible,[8–10] and they are proportional to the flexibility of the assembly, the relative flexibility as expressed by the Young's

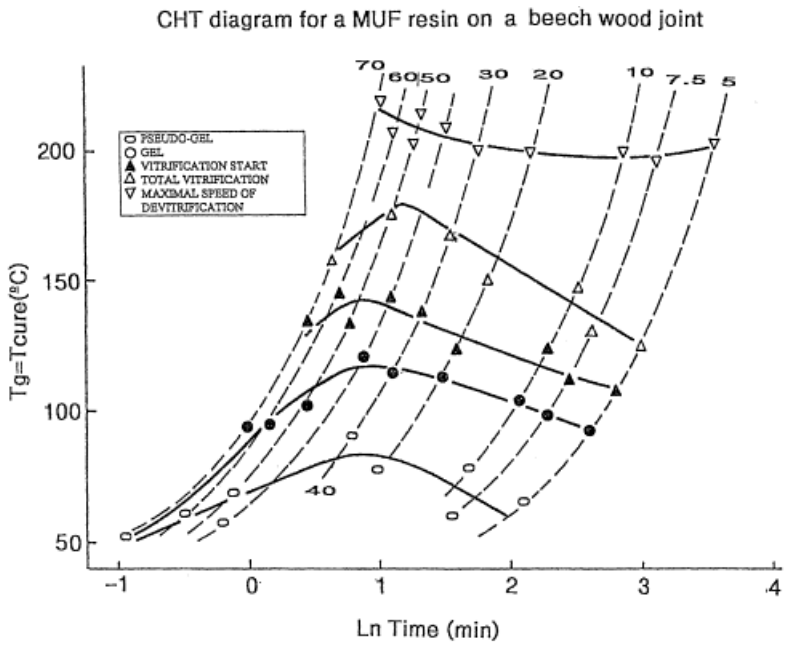

Figure 5 Detail of the modified high-temperature zone of the continuous heating transformation (CHT) diagram for a MUF resin on a beech wood joint. The experimental points, the curves of the start of and total vitrification, gelation, pseudogel, start of degradation, and maximal rate of degradation and the curves connecting them at the same heating rates are indicated.

modulus of the two primers can be calculated for the two finishes through the relationship $E_1/E_2 = \Delta f_2/\Delta f_1$. The values of Young's modulus for the resins/substrates systems were then calculated according to already reported methods according to the equation $f = km/\alpha E$, and connected regression equations that have already been reported.[8]

DISCUSSION

The water-borne state of formaldehyde based resins should entail a difference in behavior and appearance of both CHT and TTT curing diagrams in the lower temperature range of the diagrams for these resins. In the classical TTT diagram[1] for epoxy resins (not water borne) reported in the literature, the low temperature zone of the diagram is characterized by (i) the intersection of the gel and vitrification curves, the first still proceeding to a time = ∞, (ii) by a turning of the vitrification curve towards shorter times, and by (iii) its trend parallel to the time axis of the diagram (Fig. 1). In the case of water-borne PRF resins, this was not found to be the case, and the result of the trends in the lower temperature range of the diagram was found to appear as shown in Figures 2(a) and (b) and 3(a) and (b). This appears logical, as at 0°C water freezes, and the mobility of a resin in water solution is severely curtailed. In Figures 2 and 3 one can observe first of all that both gel curve and vitrification curve tend asymptotically to a time = ∞; hence, that due to the water freezing the vitrification curve does not present a turn in trend, as indicated in Figure 1. Secondly, the phenomenon of a constant T_{g0} at lower temperature does not occur, again due to the presence of the water. Thus, T_{g0} for water-borne formaldehyde resins presents itself only at a time = ∞ and corresponds to the theoretical freezing point of water. The nongelled glass domain of the the water–resin system is then quite different than what was observed for epoxy resins in the absence of solvents, which are reported in the literature. Third, a crossover point of the gel and vitrification curves does indeed occur also in the case of these formaldehyde-based, water-borne resins [Figs. 2(b) and 3(a) and (b)], but it does occur at times considerably longer than what appears in classical epoxy resins TTT diagrams.

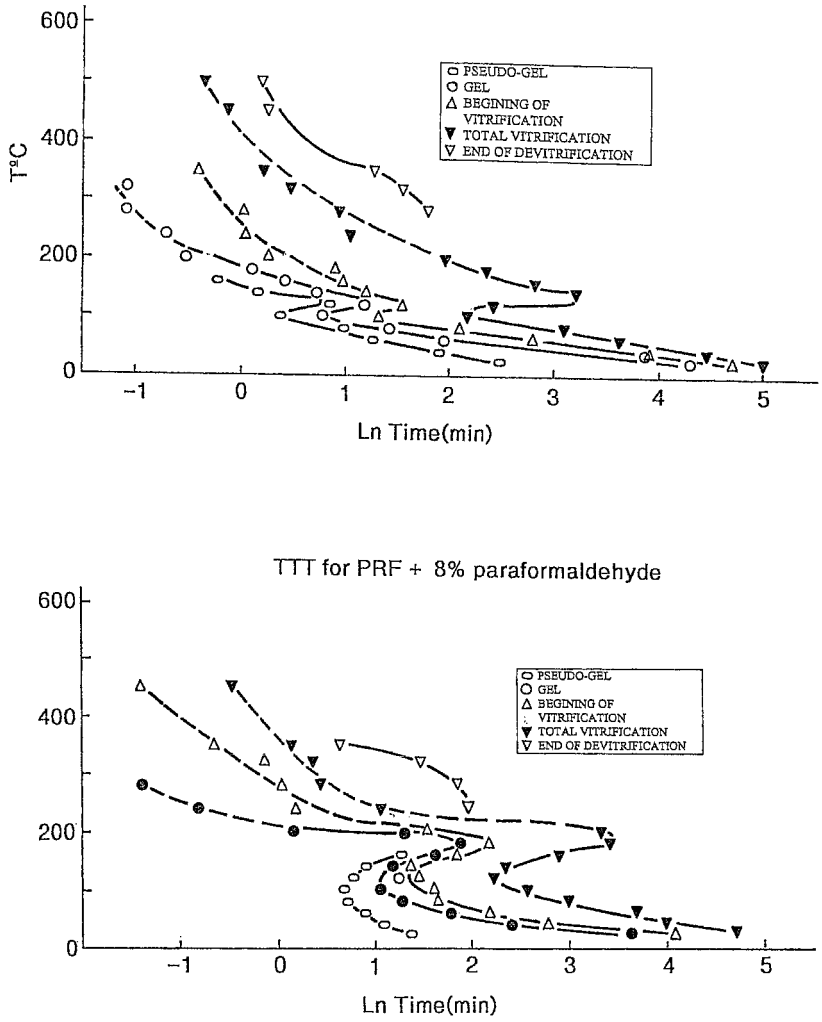

Figure 6 Detail of the modified high-temperature zone of the time–temperature–transformation (TTT) diagram for PRF resins on a beech wood joint: (a) lower viscosity, lower resorcinol content PRF resin, and (b) higher viscosity, higher resorcinol content PRF resin. The experimental points, the curves of the start of and total vitrification, gelation, pseudogel, and degradation are indicated. Continuous curves are real and due to the resin. Segmented curves are not real due to the dominant effect of substrate degradation.

Furthermore, as both gel point curve and vitrification curve tend asymptotically to a temperature of 0°C at time infinite, and the two curves are very near one to the other within a very narrow range of temperature, such a crossover point might well not be real but just a consequence of experimental error and of the mathematical extrapolation used to extend the two curves. Comparison of the details of the TTT diagrams for the two different PRF resins in Figures 2 and 3 shows that differences in behavior between the two different resins do indeed exist. Thus, the crossover points of gel and vitrification curves lie at different times and different temperature for the two PRF resins. The crossover time is shorter (ln time = 5.25) and the temperature lower (T = 16°C) for the PRF of higher viscosity and higher resorcinol content than for the resin of lower viscosity and lower resorcinol content (ln time = 9, T = 20°C). As the reactivity of the two curves as measured by their gel time were set to be very similar, the effect observed is not a consequence of lower or higher reactivity of the resin; hence, it is not caused by the lower or higher resorcinol content of the resin (although this is quite likely to have some importance in resins of different reactivi-

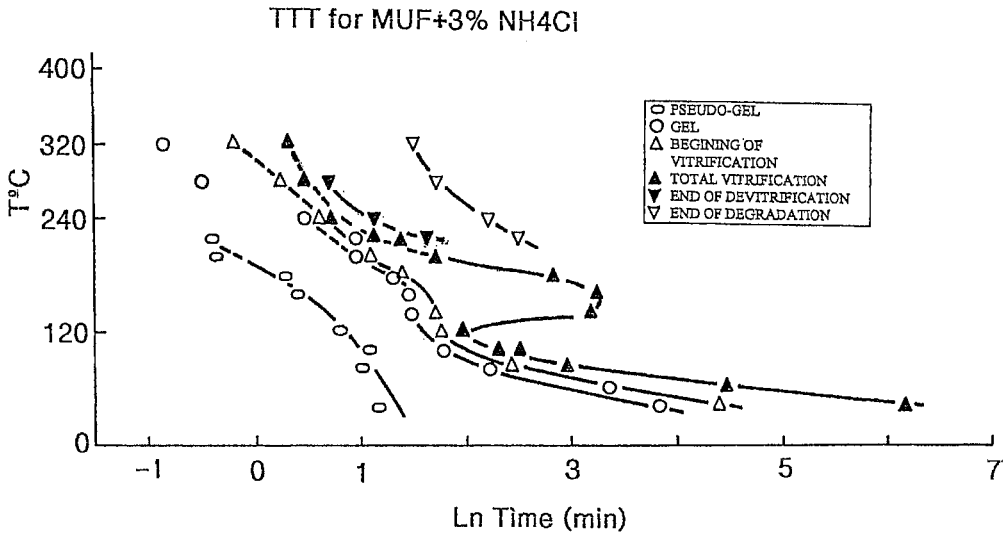

Figure 7 Detail of the modified high-temperature zone of the time–temperature–transformation (TTT) diagram for a MUF resin on a beech wood joint. The experimental points, the curves of the start of and total vitrification, gelation, pseudogel, and degradation are indicated. Continuous curve are real and due to the resin. Segmented curves are not real due to dominant effect of substrate degradation.

ties), but appears to be exclusively due to their differences in viscosity. The same is valid for the curves of the lower viscosity resin occurring at higher temperatures for the same reaction time than the curves of the higher viscosity resin. The position of the crossover point of vitrification and gelation curves becomes a debatable issue if, as shown in the figures both vitrification and gelation curves tend asymptotically to a temperature of 0°C at time = ∞.

If the crossover point is real and not due to experimental error, than a further vitrified but not gelled phase exists in a very thin domain at very long reaction times, a phase that should occur when passing from the domain of the vitrified but not gelled phase occurring at temperature ≤ 0°C through a liquid phase first. It is not the existence of this further phase that is in doubt, as this is in line with the appearance of CHT and TTT diagrams already reported for epoxy resins.[1,2] What is in question is the existence of the liquid phase between the two vitrified but not gelled domains: its existence clearly shows that the present of a solvent, in this case water, renders considerably more complex the diagram, and that the diagram can quite well indicate both the behavior of the solvent+polymer system, as well as of the solvent as a separate system from the polymer. The crossover point of the gelation and vitrification curves may well not present itself at temperatures higher than 0°C for thermosetting PF, UF, and MUF resins due to their lower reactivity relatively to PRF resins. Of these other resins, the MUF resins at least are most likely to present the crossover point at temperatures higher than 0°C, as they can present reactivity higher enough if enough catalyst is added.

Equally different trends to those reported for TTT and CHT diagrams of the epoxy resins reported in the literature occur in the higher temperature zone of the diagrams of water-borne formaldehyde-based resins hardening on a lignocellulosic substrate. In a previous article,[6] this has already been reported for both phenol–formaldehyde (PF) and urea–formaldehyde (UF) thermosetting resins, with the error, however, being committed to extrapolate from experimentally obtained CHT diagrams also the trend in TTT diagrams. The work was repeated experimentally for both CHT and TTT diagrams and for both the two resins now under investigations, namely PRF and MUF resins, with results reproducing what already was found in the case of CHT diagrams, but different results being obtained, this time experimentally, for TTT diagrams. In both cases however, both diagrams are different even in the higher temperature zone from what was reported for epoxy resins in the literature. The higher temperature zone of the CHT diagrams for the PRF resins and the MUF resin are reported in Figures

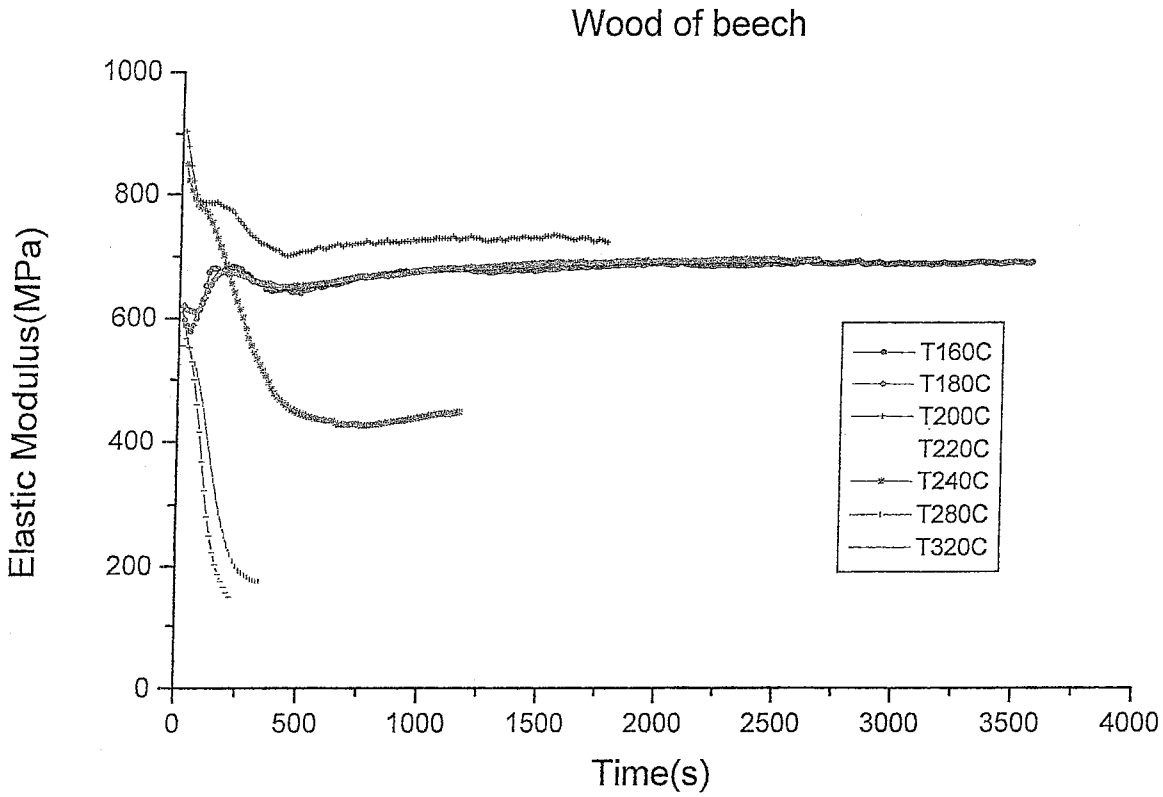

Figure 8 Variation of elastic modulus as a funcion of time of the substrate beech wood under isothermal heating at temperatures between 160 and 320°C. Note progressively more extensive degradation setting in from 220°C and at higher temperatures.

4(a) and (b) and 5, and show the same trends (and for the same reasons, namely the interactive nature of the substrate and the movement of water from resin to substrate and vice versa) observed for the UF and PF resins.

The experimental TTT diagrams shown in Figures 6(a) and (b) and 7 show, however, quite a different trend from the CHT diagrams for the same resins and for the TTT diagrams reported in the literature. To start to understand the trend shown in Figures 6 and 7 it is first necessary to observe what happens to the modulus of the wood substrate alone (without a resin being present) when examined under the same conditions of a wood joint during bonding (Fig. 8). No significant degradation occurs up to a temperature of 180°C (Fig. 8), as shown by the relative stability of the value of the elastic modulus as a function of time. Some slight degradation starts to occur at 200°C, but after some initial degradation the elastic modulus again settles to a steady value as a function of time and at a value rather comparable to the steady value obtained at lower temperatures. Evident degradation starts to be noticeable in the 220–240°C range, and this becomes even more noticeable at higher temperatures. The effect of substrate degradation on the TTT diagrams in Figures 6 and 7 can then only start to influence the trends in gel and vitrification curves at temperatures higher than 200°C, and it is for this reason that the region of the curves higher than 200°C are indicated by segmented lines in Figures 6 and 7. At a temperature $\leq$200°C, the trends observed are only due to the resin. In this range of temperature the eventual turning to longer time and stable temperature of the vitrification curve, characteristic of the TTT diagrams of epoxy resins, also becomes evident for the TTT diagrams of the water-borne PRF and MUF resins on lignocellulosic substrates, indicating that diffusion hindrance at a higher degree of conversion becomes for these resins also the determinant parameter defining reaction rate. What, however, differs from previous diagrams is that the trend of all the curves, namely gel curve, initial pseudogel (entanglement) curve, start and end of vitrification curve, is the same. In epoxy resins TTT diagrams (Fig. 1) the trend of the

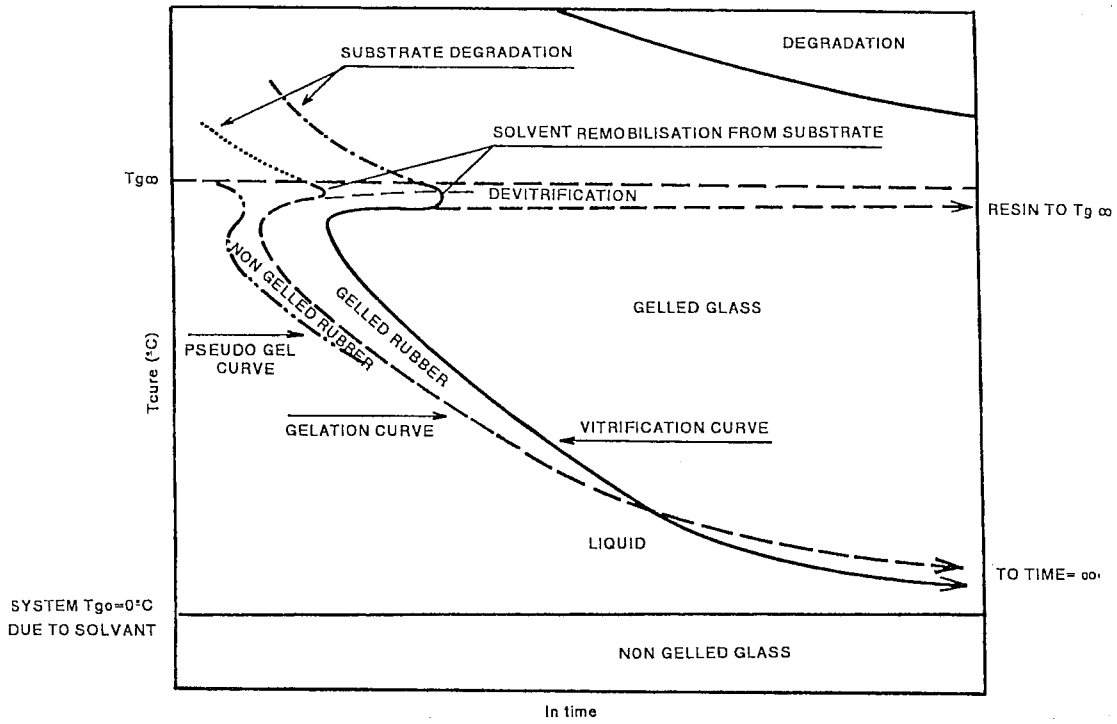

Figure 9 Modified, generalized time–temperature–transformation (TTT) diagram of water-borne PRF, MUF, UF, and PF polycondensation resins hardening on interacting lignocellulosic substrates.

gelation curve is completely different from what was reported here. The result shown in Figures 6 and 7 is, however, more logical because if diffusion problems alter the trend of the vitrification curve, then the same diffusional problem should also alter the gel and pseudogel curves. This is indeed is what the experimental results in Figures 6 and 7 indicate. It may well be that in water-borne resins the effect is more noticeable than in epoxy resins. This is the reason why it is possible to observe it in Figures 6 and 7 for PRF and MUF resins (and by inference for PF and UF resins also). With the data available and with the limitation imposed by the start of wood substrate degradation at higher temperatures it is not really possible to say if the gel curve and the vitrification curve run asymptotically towards the same value of temperature at time = ∞, although the indications are that this is quite likely to be the case. What is also evident in the trend of the two curves is the turn to the left; hence, the inverse trend of their asymptotic tendency towards $T_{g\infty}$. This turn cannot be ascribed to substrate degradation because for a very reactive resin such as the low viscosity PRF such a turn already occurs at a temperature lower than 150°C, hence, much lower than the temperature at which substrate degradation becomes significant [Figs. 6(a) and 8]. This inverse trend can only be attributed to moisture movements in the composite joint, an occurrence well known in hot cured wood panel products. Thus, water that had penetrated the substrate in the initial heating phase, for rheological reasons, at higher temperature starts coming out of the substrate and into the resin layer. This causes plasticization of the glue line due to lowering of apparent crosslinking, and is reflected in the curves trend indicating an easing of the diffusional problem already proven to occur at such a high degree of conversion.[4] It is difficult to decide if the easing of the diffusional problem in this region is real or is only an artifact of the measuring system: the indications of water movements in hot-bonded wood joints indicates that it is very real.

Two other aspects of the TTT diagrams in Figures 6 and 7 must be discussed, these being the trend of the curves at temperatures higher than 200°C and the trend of the devitrification (or resin degradation) curve. The segmented lines trend and experimental points of all the curves at temperatures higher than 200°C are clearly only an

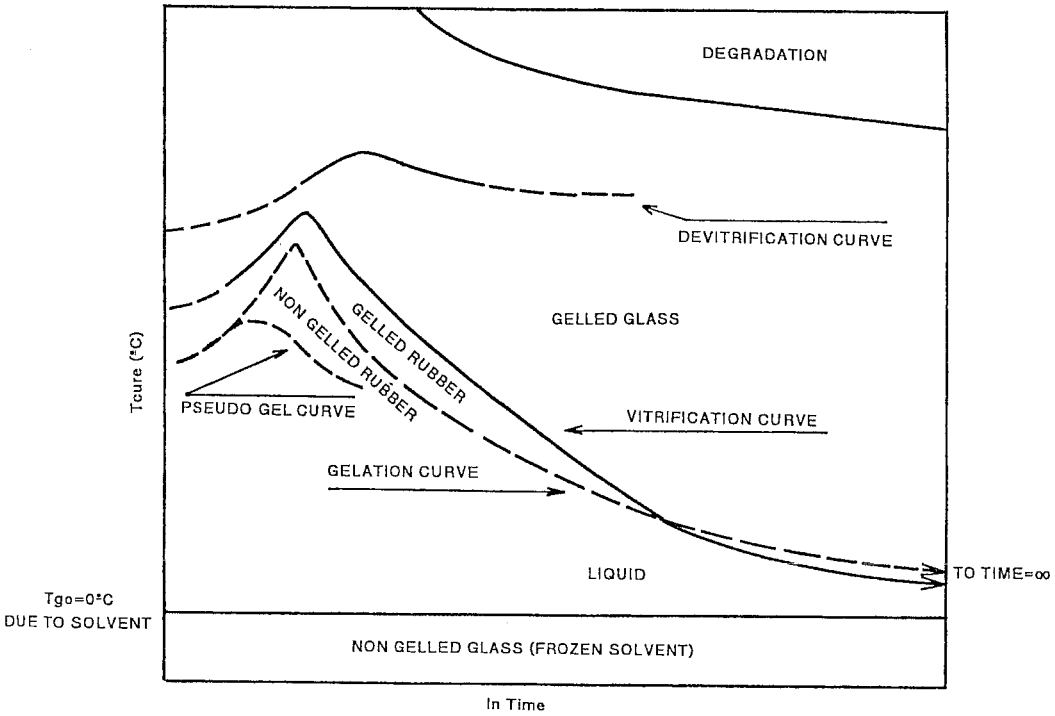

Figure 10 Modified, generalized continuous heating transformation (CHT) diagram of water-borne PRF, MUF, UF, and PF polycondensation resins hardening on interacting lignocellulosic substrates.

effect caused by the ever more severe degradation of the substrate (Fig. 8): degradation of the substrate infers a greater mobility of the polymer network constituting the substrate, hence the continuation of the curves as shown in their segmented part. That this is the case is also supported by the virtual negative times yielded by the TMA equipment when the temperature becomes extreme, as well as by the trend of the resin's higher degradation curve, which tends to intersect the vitrification curve at about 200–220°C or higher, this being a clear indication that one is measuring the changes in the reference system, the substrate itself, and that these are at this stage so much more important than the small changes occurring in the resin to be able to dominate the whole complex system, which is the bonded joint.

The CHT and TTT diagrams pertaining to water-borne formaldehyde-based polycondensation resins on a lignocellulosic substrate should then appear in their entirity as shown in Figures 9 (TTT) and 10 (CHT). The different domains pertaining to the different states of matter, namely liquid, gelled rubber, ungelled glass, and gelled glass, are, however, different than what was observed for nonsolvent borne epoxy resins.

The last question that needs answering from all the above is if the equation of Di Benedetto[11] under the form of Pascault and Williams,[12] describing T_g as a function of the degree of conversion p, namely

$$(\lambda p)/[1 - (1 - \lambda)p] = (T_g - T_{g0})/(T_{g\infty} - T_{g0})$$

is still usable on water-borne polycondensates hardened on a lignocellulosic substrate in which it has been shown that both the CHT and TTT diagrams differ from the standard model. It has already been shown[6] that $T_{g\max}$ can be substituted for $T_{g\infty}$ in the case of the CHT diagrams. The only difference is then that T_{g0} is now a fixed value, namely 0°C, this being the freezing temperature of water (it would be different if the resin is under pressure or in another solvent), for both CHT and TTT diagrams. $T_{g\infty}$ is clearly still the same in a TTT diagram, although its value is much more obscure and difficult to determine, and thus the equation should be equally valid than for non aqueous, nonsolvent systems within the limitations outlined above.

To conclude, it must be clearly pointed out that what is outlined above and the modified CHT and TTT diagrams only apply to water-borne formal-

dehyde-based polycondensates on a lignocellulosic substrate, hence, in their main use, that is for wood adhesives. If what was outlined above may be applicable to other resins on wood or on other types of interacting substrates cannot be forecast with the data available. This will, again, have to be determined experimentally for each different substrate, resin, and solvent used.

The authors wish to thank Miss C. Simon for the preparation of the PRF resins according to industrial formulations, and Mr. E. Medina for producing some of the TMA thermograms for the PRF resins.

REFERENCES

1. Enns, J. B.; Gillham, J. K. J Appl Polym Sci 1983, 28, 2831.
2. Wisanrakkit, G.; Gillham, J.K.; Enns, J. B. J Appl Polym Sci 1990, 41, 1895.
3. Montserrat, S. J Appl Polym Sci 1992, 44, 545.
4. Nunez, L.; Fraga, F.; Nunez, M. R.; Villanueva, M. J Appl Polym Sci 1998, 70, 1931.
5. Hofmann, K.; Glasser, W. G. Thermochim Acta 1990, 166, 169. (1990)
6. Pizzi, A.; Lu, X.; Garcia, R. J Appl Polym Sci 1999, 71, 915.
7. Pizzi, A. Wood Adhesives Chemistry and Technology; Dekker: New York, 1983.
8. Pizzi, A. J Appl Polym Sci 1997, 63, 603.
9. Pizzi, A. J Appl Polym Sci 1997, 65, 1843.
10. Pizzi, A.; Probst, F.; Deglise, X. J Adhesion Sci.Technol 1997, 11, 573.
11. DiBenedetto, A. T. In J Macromol Sci Rev Macromol Chem 1969, C3, 69.
12. Pascault, J. P.; Williams, R. J. J Polym Sci Phys Ed 1990, 28, 85.